Vol. 25, No. 3(2026) Mat26861

Revista Mexicana de Ingeniería Química

Experimental evaluation of detrending and spectral/time-frequency methods for electrochemical noise-based corrosion rate estimation of aluminum 6061-T6 in sulfuric acid

Evaluación experimental de técnicas de eliminación de tendencia y métodos espectrales/tiempo-frecuencia para la estimación de la velocidad de corrosión mediante ruido electroquímico en aluminio 6061-T6 en ácido sulfúrico

O.J. Ramos-Negrón[1]*, J.F. Solís-Alvarado[1], J. Uruchurtu-Chavarin[2], L. Morales-Clemente[1], and C. Reyes-del-Valle[1]

[1]Tecnológico Nacional de México / ITS de Las Choapas. Carretera Las Choapas-Cerro de Nanchital km. 6.0 Col J. Mario Rosado C.P. 96980 Las Choapas, Veracruz, México.

[2]Centro de Investigación en Ingeniería y Ciencias Aplicadas-Universidad Autónoma del Estado de Morelos, Av. Universidad 1001, Col. Chamilpa, C.P. 62209, Cuernavaca, Morelos, México.

Sent: July 29, 2026

Abstract

This work presents an experimental evaluation of detrending techniques and spectral analysis methods for estimating the corrosion rate (V_c) of aluminum 6061-T6 exposed to a 15 % w/w sulfuric acid solution. A total of 1024 electrochemical current noise (ECN) and electrochemical potential noise (EPN) records were analyzed under passive monitoring conditions. The signals were processed using a factorial combination of five preprocessing conditions: raw signal, linear detrending, polynomial detrending, wavelet detrending, and empirical mode decomposition (EMD), together with four analysis methods: statistical method (SM), fast Fourier transform (FFT), maximum entropy method (MEM), and Stockwell transform (ST). The estimates were compared with reference values obtained from Tafel polarization curves and a commercial Gamry system.

The results showed that, when all preprocessing conditions were considered, ST provided the lowest global relative error, followed by FFT, whereas MEM was strongly affected by the Raw–MEM condition. When the Raw condition was excluded and only detrended signals were analyzed, ST and MEM showed the closest agreement with the Gamry reference value, with average relative errors of 10.8 % and 11.8 %, respectively. The statistical method systematically underestimated V_c. Two-way ANOVA confirmed significant effects of detrending, analysis method, and their interaction ($p < 10^{-300}$). These findings demonstrate that the combined selection of preprocessing and spectral/time-frequency analysis is critical for obtaining reliable corrosion-rate estimates from electrochemical noise data, particularly in systems affected by drift, transient behavior, or passivation.

Keywords: Electrochemical noise, Corrosion monitoring, Detrending techniques, Time-frequency analysis (FFT, MEM, ST), ANOVA.

Resumen

En este trabajo se presenta una evaluación experimental de técnicas de eliminación de tendencia y métodos de análisis espectral para estimar la velocidad de corrosión (V_c) del aluminio 6061-T6 expuesto a una solución de ácido sulfúrico al 15 % p/p. Se analizaron 1024 registros de ruido de corriente electroquímica (ECN) y ruido de potencial electroquímico (EPN), adquiridos bajo condiciones de monitoreo pasivo. Las señales fueron procesadas mediante una combinación factorial de cinco condiciones de preprocesamiento: señal original, detrending lineal, detrending polinomial, wavelet y descomposición empírica de modos (EMD), junto con cuatro métodos de análisis: método estadístico (SM), transformada rápida de Fourier (FFT), método de máxima entropía (MEM) y transformada de Stockwell (ST). Las estimaciones se compararon con valores de referencia obtenidos mediante curvas de Tafel y un sistema comercial Gamry.

Los resultados mostraron que, al considerar todas las condiciones de preprocesamiento, ST presentó el menor error relativo global, seguido por FFT, mientras que MEM fue afectado principalmente por la condición Raw–MEM. Al excluir la condición Raw y analizar únicamente señales con detrending, ST y MEM mostraron la mayor concordancia con el valor de referencia obtenido mediante Gamry, con errores relativos promedio de 10.8 % y 11.8 %, respectivamente. El SM subestimó sistemáticamente V_c. El ANOVA de dos vías confirmó efectos significativos del detrending, del método de análisis y de su interacción ($p < 10^{-300}$). Estos hallazgos demuestran que la selección conjunta del preprocesamiento y del método espectral/tiempo-frecuencia es crítica para obtener estimaciones confiables de corrosión mediante EN, especialmente en sistemas con deriva, comportamiento transitorio o pasivación.

Palabras clave: Ruido electroquímico, monitoreo de corrosión, técnicas de eliminación de tendencia, análisis tiempo-frecuencia (FFT, MEM, ST), ANOVA.

*Corresponding author. *E-mail*: ramos-negron.oj@choapas.tecnm.mx;
https://doi.org/10.24275/rmiq/Mat26861
ISSN:1665-2738, *issn-e*: 2395-8472

1 Introduction

Since the formulation proposed by Stern and Geary 1957, its study has allowed for the establishment of criteria to understand, measure, and mitigate the deterioration of materials in service. However, its consequences remain critical: economic losses on the order of hundreds of billions of dollars have been reported in the United States *Curso de Corrosión Básica* 2004; Pierre R. Roberge 2000; Pierre R. Roberge 2008, in addition to failures with human and infrastructure impacts, such as the tragedy that occurred in Guadalajara, Jalisco, Mexico in 1992 Pierre R Roberge 2007. This background justifies the development of monitoring techniques capable of detecting and quantifying corrosive processes under real operating conditions. In this regard, recent reviews have pointed out that electrochemical methods continue to be essential for the evaluation of corrosion and protection of metallic materials, although their reliability depends on factors such as instrumentation, data processing and the interpretation model used for each system Xia *et al.,* 2022.

In this context, electrochemical noise (EN) analysis has become established as a non-invasive technique for online corrosion monitoring. The method is based on the simultaneous recording of electrochemical current noise (ECN) and electrochemical potential noise (EPN) signals, whose typical amplitudes are in the range of pA to μA and μV to mV, respectively Cottis and Turgoose 1995. Because a significant portion of the information associated with corrosive processes is concentrated at low frequencies (< 1 Hz), the measurements require sufficiently long time windows Cottis 2001. This allows for the capture of slow and transient events, but introduces difficulties associated with high dimensionality, time drift, and non-stationary behavior of the signals.

EN signals have been analyzed using time-domain statistical approaches Botana-Pedemonte *et al.,* 2002, spectral techniques such as the fast Fourier transform (FFT) Cottis and Turgoose 1995; Uruchurtu and Dawson 1987, and higher spectral resolution methods, such as the maximum entropy method (MEM) Aballe *et al.,* 1999. In aluminum alloys, recent studies have combined time-domain analysis, power spectral density, and time-frequency tools, such as Hilbert-Huang analysis, to differentiate localized and mixed corrosion processes from EN signals Martínez-Ramos *et al.,* 2023. To address the non-stationary nature of EN, time-frequency and adaptive tools have been incorporated, including the discrete wavelet transform (DWT) Avalle *et al.,* 1999, empirical mode decomposition (EMD) combined with the Hilbert spectrum Homborg, Tinga, Zhang, *et al.,* 2013, and the Stockwell transform (ST), which provides a time-frequency representation with frequency-dependent windows Ramos-Negrón, Arellano-Pérez, *et al.,* 2019. In particular, the ST has recently been proposed as an alternative for estimating the V_c of Al 6061-T6 from EN signals in media such as H_2SO_4, NaCl, and demineralized water Escobar-Jiménez *et al.,* 2023. These approaches have shown sensitivity in differentiating mechanisms such as uniform corrosion, active localized corrosion, and metastable pitting by means of the energy distribution in characteristic bands Arellano-Pérez *et al.,* 2019; Ramos-Negrón, Escobar-Jiménez, *et al.,* 2019.

In this regard, the use of the ST in conjunction with energy-based metrics, such as Shannon energy, has improved the discrimination of corrosion mechanisms Ramos-Negrón, Escobar-Jiménez, *et al.,* 2019. Likewise, the Synchrosqueezing Transform (SST) has refined time-frequency resolution and facilitated the classification of signals obtained in aggressive or mixed media Arellano-Pérez *et al.,* 2019. These advances demonstrate the potential of spectral and time-frequency methods for developing automated diagnostic schemes and, eventually, predictive corrosion systems.

However, a critical problem in EN analysis is the presence of drift, associated with long-term physical processes, reference instability, or natural system polarization. Its removal is a crucial preprocessing step, as it can alter the statistical and spectral properties of the signals and, consequently, affect the estimation of V_c. This need for robust processing aligns with recent EN-based monitoring approaches, where EPN and ECN signals are segmented and transformed into features to detect deviations from uniform corrosion conditions Abdulmutaali *et al.,* 2025. Although techniques such as least squares, polynomial regression, wavelets, and EMD have been employed, a comparative and systematic evaluation of their effect on signal integrity and the performance of estimation methods is still required.

In particular, experimental evidence jointly evaluating the effect of detrending and the analysis method on the estimation of V_c remains limited, considering not only the relative error compared to an operational reference, but also the statistical interaction between both factors. In this context, the main contribution of this work is the joint factorial evaluation of five detrending strategies and four methods for estimating V_c on an extensive experimental base of EN signals, incorporating relative error, statistical interaction, and effect sizes as methodological selection criteria.

Aluminum and its alloys exhibit a strongly medium-dependent electrochemical response due to the formation of a surface oxide/hydroxide film that can act as a protective barrier under

moderate conditions but becomes destabilized in aggressive environments. In chloride-rich media, localized film breakdown favors pitting processes; in alkaline solutions, the increased solubility of aluminum species can accelerate dissolution; and in acidic media, the competition between active dissolution, surface film formation, and regeneration can produce electrochemical transients relevant for EN analysis Ikeuba *et al.,* 2024; Lavanya *et al.,* 2024; Milošev 2024. In passivable systems exposed to sulfuric acid H_2SO_4, surface film stability has been shown to modify parameters such as I_{corr}, R_p, and electrochemical impedance Márquez-Herrera *et al.,* 2026. Therefore, 6061-T6 aluminum in H_2SO_4 at 15 % constitutes a suitable system to evaluate how drift, transients and signal preprocessing influence the estimation of V_c using EN.

This work experimentally evaluates the effect of different trend removal techniques on EN signals obtained from 6061-T6 aluminum exposed to a 15 % H_2SO_4 solution. The ECN and EPN signals are processed using five preprocessing conditions: original signal, linear detrending, polynomial detrending, wavelet detrending, and EMD detrending. Subsequently, V_c is estimated using the statistical method (SM), FFT, MEM, and ST, and the performance of each combination is compared with reference values obtained using Tafel curves and a commercial Gamry system.

The central objective is to determine how the combined selection of the detrending method and the analysis technique influences the estimation of V_c. To this end, a factorial design and a two-way ANOVA are used to quantify the main effects and the interaction between both factors. With this approach, the study seeks to provide methodological criteria for selecting preprocessing and analysis combinations that preserve relevant electrochemical information, reduce low-frequency artifacts, and improve the reliability of EN-based corrosion monitoring.

2 Materials and Methods

2.1 *Electrode preparation, electrochemical cell, and signal acquisition*

Working electrodes of 6061-T6 aluminum were used, with the following nominal composition (wt.%): Si 0.40–0.80, Fe ≤ 0.70, Cu 0.15–0.40, Mn ≤ 0.15, Mg 0.80–1.20, Cr 0.04–0.35, Zn ≤ 0.25, Ti ≤ 0.15, and Al balance. The samples were machined into a cylindrical shape, with a diameter of 6.35 mm and a length of 60 mm, and encapsulated in epoxy resin, leaving only one circular face exposed to the corrosive medium. The exposed active area was 0.3167 cm^2. The surface preparation consisted of progressive sanding with silicon carbide papers from #180 grit to #3000 grit, followed by polishing with diamond paste to obtain a mirror finish. The design of the encapsulated electrode is shown in Figure 1.

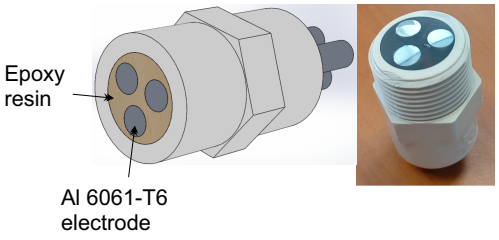

Fig. 1: Aluminum 6061-T6 working electrode encapsulated in epoxy resin.

The corrosive medium was an aqueous solution of a 15 % w/w aqueous sulfuric acid solution, maintained at an ambient temperature of approximately 25 °C. The electrodes remained fully immersed for 582.54 h, under exposure conditions without external imposition of potential or current.

The EN signals were acquired using a passive setup. A three-working-electrode configuration consisting of three nominally identical working electrodes (**WE**), identified as $\mathbf{WE_1}$, $\mathbf{WE_2}$, and $\mathbf{WE_3}$, was used. Electrochemical current noise (ECN) was recorded between $\mathbf{WE_1}$ and $\mathbf{WE_2}$ using a **Keysight 34461A** multimeter configured for current measurement, while electrochemical potential noise (EPN) was measured differentially between $\mathbf{WE_1}$ and $\mathbf{WE_3}$ using an **Agilent 34401A**. In this configuration, ECN represents spontaneous current fluctuations associated with local corrosion processes, while EPN reflects spontaneous system potential variations.

Fig. 2 shows the cell schemes considered for the acquisition of EN; in this study scheme (d) was used, corresponding to a configuration of three nominally identical working electrodes with differential measurement.

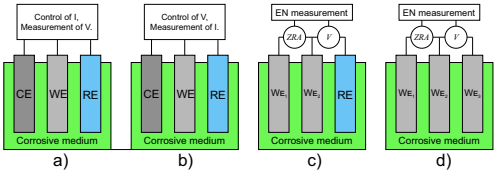

Fig. 2: Electrochemical cell configuration schemes for EN acquisition Cottis 2001. Scheme (d) with three nominally identical **WE** and differential measurement was used.

The geometric arrangement of the electrodes on the exposed surface was linear, as shown in Fig. 3(a), for the purpose of maintaining a defined separation between electrodes and reducing uncontrolled geometric effects during measurement.

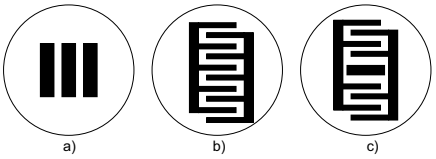

Fig. 3: Different geometric configurations of electrodes at the exposed end. In this study, the linear configuration (a) was used.

Both multimeters were connected to a computer via USB interface and controlled in LabVIEW 2012. The ECN and EPN signals were acquired at a sampling frequency of 2 Hz, equivalent to a sampling interval of 0.5 s. 1024 individual EN records were acquired, each with 4096 data points per channel, corresponding to a duration of 2048 s, or approximately 34.13 min per recording. With this time window, the frequency resolution was 0.488 mHz, while the maximum analyzable frequency was 1 Hz, according to the Nyquist criterion.

The 1024 recordings were treated as individual time windows acquired during the electrochemical exposure. Therefore, these records allow the temporal variability and robustness of the V_c estimators to be evaluated, but should not be interpreted as independent electrochemical replicates of different cells.

2.2 *Signal preprocessing*

The EPN and ECN signals were processed in volts (V) and amperes (A), respectively. To obtain a comparable magnitude between recordings, the current was normalized with respect to the exposed active area of the electrode, calculating the noise current density as:

$$J_{CN} = \frac{I_{CN}}{A} \quad \left[\frac{\text{A}}{\text{cm}^2}\right], \tag{1}$$

where I_{CN} is the electrochemical noise current signal and A is the exposed active area of the electrode. From this normalization, the magnitudes R_n and Z_n were interpreted as area-normalized resistances or impedances, so that the corrosion current density i_{corr} is expressed in A/cm^2.

Prior to statistical, spectral, and time–frequency analysis, each EPN and ECN record was subjected to a detrending process. This step is necessary because EN signals can contain low-frequency components associated with instrumental drift, slow evolution of corrosion potential, surface adsorption, corrosion product formation, or passivation processes. If these components are not adequately removed, they can alter the variance, contaminate the power spectral density, and bias the V_c estimate.

In this work, five preprocessing conditions were evaluated: uncorrected original signal (*Raw*), linear detrending, polynomial detrending, detrending using discrete wavelet transform, and detrending using empirical mode decomposition (EMD). In all cases, the corrected signal was generally obtained as:

$$y_{corr}(t) = y(t) - \hat{y}_{trend}(t), \tag{2}$$

where $y(t)$ represents the original EPN or ECN signal, $\hat{y}_{trend}(t)$ is the trend estimated by each method and $y_{corr}(t)$ is the corrected signal used for the subsequent calculation of R_n, Z_n, and V_c.

For the Raw condition, the EPN and ECN signals were analyzed without trend removal. In the linear case, $\hat{y}_{trend}(t)$ was estimated using a first-order least squares fit. For the polynomial method, time was normalized as $t_{norm} = (t - \bar{t})/\sigma_t$ and the trend was approximated by a 5th-degree polynomial. In the wavelet approach, a mother wavelet `sym8` with decomposition level 8 was used; the level 8 approximation was considered a slow component and was subtracted from the original signal. For EMD, the signal was represented as the sum of intrinsic mode functions (IMFs) and a low-frequency residual.

$$x(t) = \sum_{k=1}^{K} IMF_k(t) + r(t), \tag{3}$$

where $r(t)$ represents the slow component associated with the drift. The corrected signal was reconstructed by removing this residual and retaining the relevant oscillatory components. The implementation of EMD was carried out using the MATLAB `emd` function, using its internal decomposition criteria.

Table 1 summarizes the methods considered, their operating principle, advantages, limitations, and representative references.

The quantitative comparison of these preprocessing conditions was subsequently performed based on their effect on the estimation of V_c, the dispersion of the results and their interaction with the SM, FFT, MEM, and ST analysis methods.

2.3 *Corrosion rate calculation*

The V_c was estimated from the EPN and ECN signals using four approaches: time-domain statistical method, FFT, MEM, and ST. In all cases, the estimate was based on an equivalent electrochemical quantity—noise resistance, spectral impedance, or time-frequency impedance—from which the corrosion current density was calculated using the Stern and Geary relation:

$$i_{corr} = \frac{B}{R_{eq}}, \tag{4}$$

where R_{eq} represents R_n, $\overline{Z_n}$ or $\overline{\psi_n}$, depending on the method used. The Stern and Geary constant was obtained from the anodic β_a and cathodic β_c slopes determined by Tafel curves:

Table 1: Detrending methods applied to EN signals.

Method	Applied principle	Main advantage	Critical limitation	References
Raw	The signal is analyzed without trend removal.	Preserves the measured signal entirely and serves as the baseline condition.	May overestimate low-frequency energy and bias R_n, PSD, or Z_n.	U. Bertocci *et al.,* 2002; Cottis 2001; Lentka and Smulko 2019
Linear	Fitting and subtraction of a first-order trend using least squares.	Low computational cost and easy implementation.	Insufficient when the drift exhibits curvature or nonlinear changes.	U. Bertocci *et al.,* 2002; Cottis 2001; Lentka and Smulko 2019
Polynomial	Fitting of a fifth-degree polynomial using normalized time.	Captures moderate curvature and reduces low-frequency components.	May induce overfitting or remove useful electrochemical information if the order is not properly selected.	U. Bertocci *et al.,* 2002; Havashinejadian *et al.,* 2017; J. Y. Huang *et al.,* 2010
Wavelet	Multiresolution decomposition using the `sym8` wavelet; the level-8 approximation is subtracted as the trend.	Suitable for nonstationary signals and localized transients.	Depends on the mother wavelet, decomposition level, and reconstruction criterion.	Aballe *et al.,* 1999; Homborg, Tinga, Westing, *et al.,* 2014; J. Y. Huang *et al.,* 2010
EMD	Adaptive decomposition into IMFs and a low-frequency residual; the residual is subtracted as the trend.	Does not require a fixed basis and adapts to nonlinear/nonstationary signals.	Sensitive to noise, mode mixing, and the IMF selection criterion.	Homborg, Tinga, Zhang, *et al.,* 2013; N. E. Huang *et al.,* 1998; Lentka and Smulko 2019

$$B = \frac{\beta_a|\beta_c|}{2.303(\beta_a + |\beta_c|)}. \tag{5}$$

In this work, $\beta_a = 190.6\,\text{mV/dec}$, and $\beta_c = -599.7\,\text{mV/dec}$ were used; for the calculation of B, the absolute magnitude of the cathodic slope was used, obtaining $B = 62.8\,\text{mV}$. Subsequently, V_c was calculated using the expression based on Faraday's law:

$$V_c = k\, i_{\text{corr}} \left(\frac{W_{\text{eq}}}{\rho}\right), \tag{6}$$

where $k = 3.27 \times 10^{-3}$ is the conversion factor used to express V_c in *mm/year*, W_{eq} is the equivalent weight of the material, and ρ is its density. For 6061-T6 aluminum, $W_{\text{eq}} = 9.01\,\text{g/mol}$ and $\rho = 2.7\,\text{g/cm}^3$ were considered.

Under this framework, perturbative and quasi-stationary techniques, such as potentiodynamic polarization, electrochemical impedance spectroscopy (EIS), and linear polarization resistance (LPR), remain reference tools for evaluating corrosion resistance, estimating kinetic parameters, and comparing trends obtained using non-perturbative methods. Several studies published in the Mexican Journal of Chemical Engineering have employed these techniques to analyze anticorrosive coatings, corrosion inhibitors, protective film formation, and electrochemical response in aggressive media Cano *et al.,* 2023; Esquivel-Rojas *et al.,* 2020; Márquez-Herrera *et al.,* 2026. In the present investigation, these techniques are considered as a complementary electrochemical framework: Tafel curves were used to obtain the slopes β_a and β_c required in the Stern and Geary 1957 constant, while the main comparison between methods was carried out based on the EN signals.

Due to the frequency discretization imposed by $F_s = 2\,\text{Hz}$, and $N = 4096$, the effective bandwidth for FFT and ST corresponded approximately to the interval from 3.418 mHz to 9.766 mHz. In MEM, the spectral density was estimated on a one-sided frequency grid of 1024 points, ranging from the zero-frequency component to the Nyquist frequency, i.e., from 0 to 1 Hz. Therefore, the effective frequency band used for the calculation corresponded approximately to the interval from 3.910 mHz to 9.775 mHz.

In FFT, a Hann window was applied to each signal before estimating the one-sided power spectral densities. The window was defined as

$$w[n] = 0.5\left(1 - \cos\left(\frac{2\pi n}{N-1}\right)\right), \quad n = 0, 1, \ldots, N-1, \tag{7}$$

where N is the number of samples in each record. The one-sided PSDs of the EPN and ECN signals were then estimated. For MEM, the PSDs were estimated using an autoregressive model of order $M = 200$. In ST, the time-frequency representation of the signals was obtained, and the ratio between the time-frequency magnitudes of EPN and ECN within the band of interest was averaged.

Table 2 summarizes the base magnitudes, key equations, and references used for each method.

For the comparison of EN-based methods, the $V_{c,\text{ref}} = 0.8539\,mm/year$ value, obtained using the Gamry system in EN mode, was used as the operational reference. The V_c obtained using Tafel curves was considered a complementary electrochemical reference, since this technique involves an external perturbation of the system and can temporarily modify the surface state of the aluminum. Therefore, Tafel was used to determine the slopes β_a, and β_c and the constant B, while $V_{c,\text{ref}}$ was used to calculate the relative errors of the EN methods.

Table 2: Summary of the methods used for calculating V_c.

Method	Base quantity	Equation used	References
SM	Noise resistance R_n	$R_n = \sigma_V/\sigma_J, \quad i_{\text{corr}} = B/R_n$	ASTM International 2023; Cottis 2001; Cottis and Turgoose 1995
FFT	Average noise impedance $\overline{Z_n}$	$Z_n(f) = \sqrt{\Psi_V(f)/\Psi_J(f)}, \quad \overline{Z_n} = \frac{1}{f_2-f_1}\sum_{f=f_1}^{f_2} Z_n(f)\Delta f, \quad i_{\text{corr}} = B/\overline{Z_n}$	Botana-Pedemonte *et al.*, 2002; Cottis and Turgoose 1995; Uruchurtu and Dawson 1987
MEM	Average spectral impedance $\overline{Z_n}$	$\Psi(f) = \frac{2\Delta t P_0}{\left\lvert 1+\sum_{k=1}^{M} P_k e^{-j2\pi f k\Delta t}\right\rvert^2}, \quad M = 200, \quad i_{\text{corr}} = B/\overline{Z_n}$	Aballe *et al.*, 1999; Ugo Bertocci *et al.*, 1998; Schauer *et al.*, 1998
ST	Average time–frequency impedance $\overline{\psi_n}$	$\psi_n(t,f) = \zeta_V(t,f)/\zeta_J(t,f), \quad \overline{\psi_n} = \frac{1}{f_2-f_1}\sum_f \left(\frac{1}{N}\sum_t \psi_n(t,f)\right)\Delta f, \quad i_{\text{corr}} = B/\overline{\psi_n}$	Escobar-Jiménez *et al.*, 2023; Ramos-Negrón, Arellano-Pérez, *et al.*, 2019; Stockwell *et al.*, 1996

2.4 *Statistical analysis*

To evaluate the effect of preprocessing and analysis method on the estimated V_c, a two-way ANOVA with interaction was applied, an approach widely used in factorial designs to quantify main effects and interactions between experimental factors Box *et al.*, 2005; Montgomery 2012. The first factor corresponded to the trend removal method, with five levels: Raw, Linear, Polynomial, Wavelet, and EMD; while the second corresponded to the estimation method, with four levels: SM, FFT, MEM, and ST. Therefore, each of the 1024 records was evaluated under 20 methodological combinations, generating a total of 20480 V_c estimates.

The statistical model used was:

$$V_{c,ijk} = \mu + \alpha_i + \beta_j + (\alpha\beta)_{ij} + \epsilon_{ijk}, \tag{8}$$

where $V_{c,ijk}$ is the V_c estimated for the k-th time window under the i-th detrending method and the j-th analysis method; μ is the overall mean; α_i represents the effect of the detrending method; β_j the effect of the analysis method; $(\alpha\beta)_{ij}$ the interaction between both factors; and ϵ_{ijk} the residual term.

The hypotheses evaluated were the absence of a significant effect of the detrending method, the analysis method, and the interaction between the two factors. The analysis was performed in MATLAB using the long table of results, with a significance level of $\alpha = 0.05$. Due to the large number of observations, the statistical interpretation was supplemented with effect sizes, calculated as η^2 and η_p^2, to estimate the relative contribution of each source of variation. Multiple comparisons were also considered using Tukey's post-hoc tests when significant differences were identified Montgomery 2012; Tukey 1949.

The assumptions of normality of residuals and homogeneity of variances were assessed using diagnostic tests and graphical review of the residuals. However, since EN signals can exhibit non-stationary behavior and distributions affected by electrochemical transients, the ANOVA results were interpreted in conjunction with effect sizes, interaction plots, and the relative error map.

3 Results and discussion

3.1 *Reference electrochemical characterization*

The reference electrochemical characterization was obtained using Tafel curves and measurements performed with a commercial Gamry system, in order to establish a comparative criterion for the V_c estimates obtained from EN. From the polarization curves, the anodic and cathodic Tafel slopes were determined as $\beta_a = 190.6\,\text{mV/dec}$ and $\beta_c = -599.7\,\text{mV/dec}$, respectively. Using the Stern and Geary relation described in Section *2.3*, a V_c value of 4.458 *mm/year* was obtained. However, the value adopted as the main reference for comparing EN-based methods was $V_{c,\text{ref}} = 0.8539\,mm/year$, determined using the Gamry system under EPN and ECN acquisition conditions.

The difference between the corrosion rate estimated from Tafel analysis and the reference based on EN should be interpreted considering the nature of each technique. Polarization curves imply an external perturbation of the system, and therefore can temporarily modify the surface state of the aluminum. In contrast, EN records spontaneous fluctuations under natural exposure conditions, which is especially relevant in passivable alloys, where the formation, breakdown, and regeneration of surface films can generate transient and non-steady-state responses Cottis 2001; Cottis and Turgoose 1995.

Therefore, the comparison with Tafel was interpreted as a complementary electrochemical reference, while $V_{c,\text{ref}}$ obtained by EN/Gamry was used as an operational reference to evaluate the response of the EN-based methods.

3.2 Estimation of corrosion rate using EN methods

Each of the 1024 EN records was processed using the combinations defined in the methodology: five preprocessing conditions and four methods for estimating V_c. Figure 4 shows the evolution of V_c obtained using the SM, FFT, MEM, and ST methods. Each point corresponds to the estimate performed on an individual record of EPN and ECN signals.

In general, the SM method showed the lowest values and the greatest relative dispersion, with estimates frequently below 0.5 *mm/year*. This behavior may be associated with the sensitivity of the $R_n = \sigma_V/\sigma_I$ calculation to residual drift, variance changes, and low-frequency components in signals that are not strictly stationary Cottis 2001; Cottis and Turgoose 1995. In contrast, the FFT, MEM, and ST spectral methods showed average values closer to the reference value $V_{c,\mathrm{ref}} = 0.8539\,mm/year$, suggesting a greater capacity to represent the dominant electrochemical response within the analyzed frequency range.

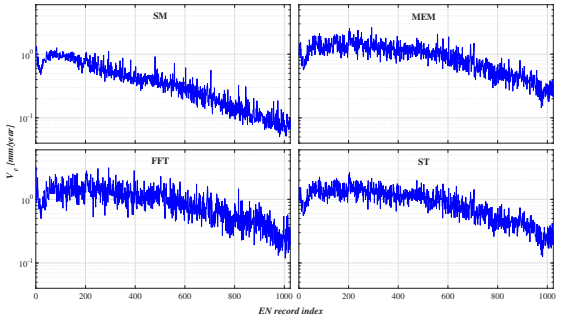

Fig. 4: Each point corresponds to the V_c estimate obtained from one EN record.

Table 3 summarizes the mean, standard deviation, observed range, and relative error of V_c for each analysis method, considering the five preprocessing conditions evaluated: Raw, linear, polynomial, wavelet, and EMD. This initial comparison allows us to observe the overall performance of each technique within the full factorial design. In this case, ST presented the lowest overall relative error, with 12.2 %, followed by FFT with 14.5 %. The SM method showed the greatest underestimation of V_c, with a relative error of 51.5 %, confirming its high sensitivity to drift, variance changes, and low-frequency nonstationary components.

Table 3: Average V_c estimated using the EN analysis methods considering the five preprocessing conditions evaluated: Raw, linear, polynomial, wavelet, and EMD. The relative error was calculated with respect to $V_{c,\mathrm{ref}} = 0.8539\,mm/year$.

Method	$\overline{V_c}$ (*mm/year*)	Std. Dev. (*mm/year*)	Range (*mm/year*)	Rel. error (%)
SM	0.414	0.300	0.038–2.628	51.5
FFT	0.978	0.539	0.112–3.250	14.5
MEM	1.141	0.589	0.102–2.669	33.6
ST	0.958	0.474	0.107–3.116	12.2

The overall average MEM value was primarily affected by the Raw–MEM condition, in which the presence of unremoved slow components increased the V_c estimate. Therefore, MEM should not be interpreted as a preprocessing-independent method, but rather as a spectral technique whose performance depends on how drift and low-frequency components not directly associated with the steady-state corrosive response are attenuated. This observation is relevant because it anticipates the statistical interaction between the detrending method and the analysis method.

To isolate the performance of the methods when an explicit trend removal step is applied, Table 4 presents the summary excluding the Raw condition. Under this comparison, MEM and ST showed the best agreement with $V_{c,\mathrm{ref}}$, with relative errors of 11.8 % and 10.8 %, respectively. This indicates that the spectral and time–frequency methods provide more consistent estimates when the signals are pre-corrected to reduce drift, without removing relevant electrochemical fluctuations.

Table 4: Average V_c estimated using the EN analysis methods excluding the Raw condition. This table summarizes the performance of the methods when an explicit detrending step was applied. The relative error was calculated with respect to $V_{c,\mathrm{ref}} = 0.8539\,mm/year$.

Method	$\overline{V_c}$ (*mm/year*)	Std. Dev. (*mm/year*)	Rel. error (%)
SM	0.402	0.302	53.0
FFT	0.978	0.540	14.5
MEM	0.954	0.469	11.8
ST	0.946	0.477	10.8

The comparison between Tables 3 and 4 demonstrates that the reliability of the V_c estimate depends not only on the analysis algorithm but also on the preprocessing stage. In particular, ST maintained the best overall performance and retained a low deviation from the reference value when only signals with detrending were considered. MEM, for its part, showed competitive performance after removing the trend but was more sensitive to the Raw condition. In

contrast, SM maintained a systematic underestimation, even after preprocessing, which limits its use as the primary method for this system.

From an electrochemical standpoint, these results are consistent with the expected behavior of a passivable alloy exposed to an acidic medium. In 6061-T6 aluminum, the EN signals can contain contributions associated with active dissolution, surface film formation, breakdown, and regeneration, as well as localized transients. Under these conditions, the direct calculation of $R_n = \sigma_V/\sigma_J$ can be affected by variance changes and residual drift. In contrast, FFT, MEM, and ST methods allow for the analysis of the relationship between the spectral components of EPN and ECN within a predefined low-frequency band, partially reducing the influence of global signal fluctuations.

The difference between the Tafel estimate and those obtained using EN must be interpreted considering the nature of each technique. Polarization curves induce an external perturbation that can temporarily modify the surface state of aluminum, while EN records spontaneous fluctuations under natural exposure conditions ASTM International 2023; Cottis 2001; Stern and Geary 1957. For this reason, the V_c obtained using Tafel is considered a complementary electrochemical reference, while the value obtained with the Gamry system in EN mode, $V_{c,\mathrm{ref}} = 0.8539\,mm/year$, is maintained as the operational reference for comparing EN-based methods. In this context, ST and MEM with detrending proved particularly suitable for representing localized or transient spectral contributions Ugo Bertocci *et al.,* 1998; Escobar-Jiménez *et al.,* 2023; Stockwell *et al.,* 1996.

This interpretation shows that the estimated V_c depends on the calculation model, the time scale considered, and the experimental system evaluated. For these reasons, the comparison between methods must be carried out within a well-defined methodological framework, avoiding interpreting as direct equivalents the values obtained using perturbative techniques, commercial EN signals, and spectral estimators derived from specific preprocessing Rodríguez-Yáñez *et al.,* 2022.

3.3 Effect of detrending and analysis method on V_c

Fig. 5 shows the distribution of V_c for the 20 combinations of detrending methods and analysis techniques. This representation allows for the simultaneous evaluation of the effect of preprocessing and the response of each method to EN signals with drift, transients, or non-stationary behavior.

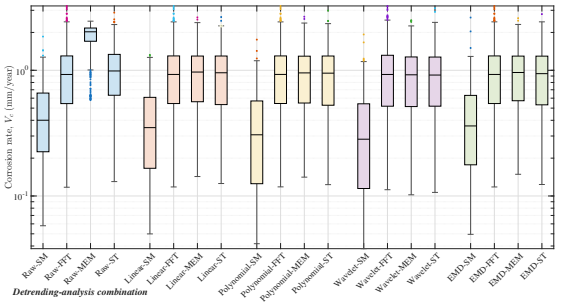

Fig. 5: Distribution of V_c by combination of detrending method and analysis technique.

The SM showed the greatest sensitivity to preprocessing, with V_c values lower than those obtained by FFT, MEM, and ST. This behavior confirms the previously observed underestimation and can be attributed to the direct dependence of $R_n = \sigma_V/\sigma_J$, a parameter susceptible to changes in variance, residual drift and low frequency components that do not necessarily represent stationary corrosive activity Cottis 2001; Cottis and Turgoose 1995; Lentka and Smulko 2019.

In contrast, spectral and time–frequency methods showed a more stable response to the type of detrending applied. Combinations based on MEM and ST showed distributions closer to the reference value $V_{c,\mathrm{ref}} = 0.8539\,mm/year$, with less relative dispersion. This suggests that analysis based on EPN and ECN spectral densities within the selected frequency range reduces the influence of global signal fluctuations and improves the consistency of the V_c estimate Ugo Bertocci *et al.,* 1998; Escobar-Jiménez *et al.,* 2023; Schauer *et al.,* 1998.

The effect of detrending was particularly evident in MEM and SM, although for different reasons. In MEM, the Raw condition produced a considerable increase in V_c, indicating that this method is sensitive to unremoved slow components when applied directly to uncorrected signals. In SM, the direct dependence of the variance of EPN and ECN maintained a systematic underestimation even after preprocessing. For its part, FFT showed a virtually constant response to the type of detrending, while ST showed the most stable overall behavior.

Taken together, these results show that the estimation of V_c depends not only on the analysis method but also on its combination with the applied preprocessing. The combinations with the lowest relative error were Wavelet–MEM and Wavelet–ST, followed by Polynomial–ST, EMD–ST, and Polynomial–MEM. Therefore, in EN signals with drift or passivating behavior, the use of appropriate detrending strategies, particularly those based on multiscale or adaptive approaches, along with spectral or time-frequency methods, is methodologically more reliable than the exclusive use of SM or the application

of MEM to Raw signals Aballe *et al.,* 1999; Homborg, Tinga, Zhang, *et al.,* 2013; Lentka and Smulko 2019.

3.4 Statistical analysis and interaction between factors

To quantify the influence of the detrending method and the analysis method on the estimation of V_c, a two-way ANOVA with interaction was applied. This approach allows for the evaluation of the main effects of each factor and the determination of whether the performance of an analysis method depends on the preprocessing applied to the EN signals Box *et al.,* 2005; Montgomery 2012. Table 5 summarizes the results obtained and includes the effect sizes η^2 and η_p^2, in order to complement the interpretation based solely on statistical significance.

The ANOVA results confirmed statistically significant effects of the detrending method, the analysis method, and the interaction between these two factors on the estimated values of V_c (Table 5). However, due to the large number of observations, the interpretation should not be based solely on the significance values. For this reason, the effect sizes allow us to assess the relative contribution of each source of variation. The analysis method was the dominant factor, with $\eta^2 = 0.2397$, indicating that it explained approximately 24.0 % of the total variability. The detrending method made a smaller, though statistically significant, contribution, with $\eta^2 = 0.0358$, equivalent to approximately 3.6 % of the total variability.

The detrending × analysis interaction was also significant and explained approximately 7.7 % of the total variability ($\eta^2 = 0.0768$). This result is methodologically relevant, as it demonstrates that the performance of each analysis technique cannot be evaluated independently of the applied preprocessing. In practical terms, the same technique can improve or degrade its accuracy depending on how drift and slow components are removed from the EPN and ECN signals. This behavior is consistent with the sensitivity of EN to instrumental drift, low-frequency components, and non-stationary processes associated with the formation, disruption, or regeneration of surface films Cottis 2001; Homborg, Tinga, Westing, *et al.,* 2014; Lentka and Smulko 2019.

Figure 6 presents the interaction graph between the detrending methods and the analysis techniques. The lack of parallelism between the curves visually confirms the interaction detected by the ANOVA. The most pronounced behavior is observed in MEM, whose V_c estimate increases considerably under the Raw condition, while after applying detrending, its values approach the range obtained with ST. For its part, FFT showed a practically constant behavior with respect to the type of preprocessing, while SM maintained values below $V_{c,\mathrm{ref}}$ in all the evaluated conditions.

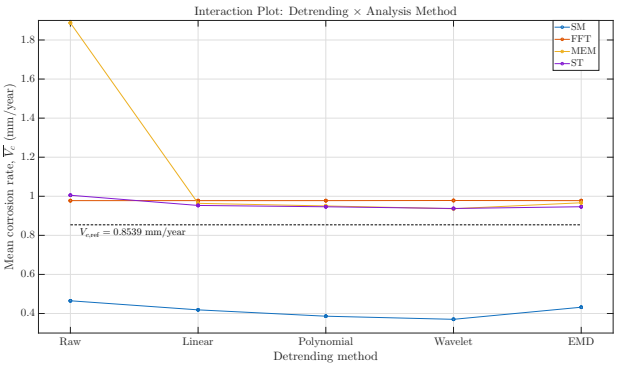

Fig. 6: Interaction graph between detrending method and analysis method. The response variable corresponds to the mean V_c. The horizontal line indicates the reference value $V_{c,\mathrm{ref}} = 0.8539\,mm/year$.

To complement the statistical analysis, Fig. 7 shows the percentage relative error with respect to the reference value $V_{c,\mathrm{ref}}$ for each detrending–analysis method combination. This representation allows the configurations with the best performance to be directly identified. The Wavelet–MEM and Wavelet–ST combinations presented the lowest relative errors, followed by Polynomial–ST, EMD–ST and Polynomial–MEM. In contrast, Raw–MEM showed the largest relative error, confirming that MEM is particularly sensitive to the presence of unremoved slow components. Likewise, the combinations associated with SM maintained high errors in all conditions, evidencing the limitation of the direct statistical approach for this system.

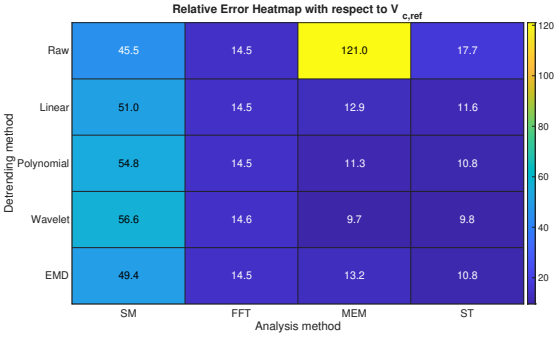

Fig. 7: Heatmap of the percentage relative error with respect to $V_{c,\mathrm{ref}}$ for each detrending–analysis method combination. Lower values indicate closer agreement with the reference value.

Taken together, the ANOVA, interaction plot, and relative error map demonstrate that reliable estimation of V_c requires joint selection of the preprocessing method and the analysis technique. The results favor the use of ST and MEM when combined with appropriate detrending strategies, particularly those

Table 5: Results of the two-way ANOVA applied to the estimated V_c values. Effect sizes η^2 and η_p^2 are included to evaluate the practical relevance of each source of variation.

Source of variation	**SS**	**df**	**MS**	**F**	p	η^2	η_p^2
Detrending method	229.86	4	57.47	283.03	2.85×10^{-237}	0.0358	0.0524
Analysis method	1537.35	3	512.45	2523.91	$< 10^{-300}$	0.2397	0.2701
Detrending × analysis	492.57	12	41.05	202.17	$< 10^{-300}$	0.0768	0.1060
Residual error	4154.16	20460	0.203	–	–	0.6477	–
Total	6413.95	20479	–	–	–	–	–

that reduce the influence of slow components without eliminating relevant electrochemical fluctuations. However, the behavior of Raw–MEM shows that MEM should not be considered robust against uncorrected signals. This evidence supports the need to consider the interaction between factors as a methodological criterion in EN-based corrosion studies.

4 Conclusions

This study comparatively evaluated the effects of preprocessing and analysis method on the estimation of V_c for 6061-T6 aluminum exposed to a 15 % w/w H_2SO_4 solution, using EPN and ECN signals. To this end, 1024 experimental records were analyzed using a factorial combination of five detrending conditions: Raw, Linear, Polynomial, Wavelet, and EMD, and four estimation methods: SM, FFT, MEM, and ST. This strategy allowed for the evaluation not only of the individual performance of each technique but also of the interaction between the applied preprocessing and the analysis method used.

The results demonstrated that both spectral and time-frequency methods provide more consistent estimates of V_c than the direct SM. Considering all preprocessing conditions, ST showed the lowest overall relative error. When the Raw condition was excluded and only detrended signals were analyzed, MEM and ST showed the best agreement with the reference value obtained using the Gamry system in EN mode ($V_{c,\mathrm{ref}} = 0.8539\,mm/year$). This greater stability is attributed to the fact that both methods allow for the analysis of the spectral contribution of the EPN and ECN signals within the frequency range of interest, reducing the influence of global fluctuations, residual drift, and non-stationary components.

The SM, although simple and computationally inexpensive, proved to be the least reliable for this system. Its estimates tended to underestimate V_c and showed greater sensitivity to preprocessing. This confirms that the direct calculation of noise resistance, based on the relationship $R_n = \sigma_V/\sigma_I$, can be affected by variance changes, low-frequency drift, and non-stationary transients. Therefore, its use as the primary diagnostic tool should be limited to sufficiently stable conditions or as a preliminary reference.

Signal preprocessing had a significant effect on the V_c estimation. Raw, Linear, and Polynomial techniques provided a useful baseline for comparison; however, nonparametric methods, primarily Wavelet and EMD, performed better when combined with MEM or ST. These techniques allowed for the attenuation of slow components associated with drift without excessively suppressing relevant electrochemical fluctuations. This result is particularly important in passivable materials such as 6061-T6 aluminum, where the formation, breakdown, and regeneration of surface films can generate transient and non–steady–state signals.

The two–way analysis of variance confirmed that both the detrending method and the analysis method significantly influence the estimated V_c values. The analysis method was the dominant factor, while detrending made a smaller but statistically significant contribution. Furthermore, the interaction between these two factors was highly significant, demonstrating that the performance of an analysis technique should not be evaluated in isolation, but rather in conjunction with the applied preprocessing. This finding is one of the main contributions of this work, as it highlights that methodological selection in EN studies should be carried out in a combined manner, rather than sequentially or independently.

Comparison with the values derived from Tafel showed significant differences compared to the estimates based on EN. Although polarization curves constitute a standard electrochemical technique, their perturbative nature can induce responses different from those observed under natural exposure conditions. In this study, the V_c estimated using Tafel was considerably higher than the reference value obtained by EN/Gamry, which reinforces the need to interpret both techniques as complementary and not necessarily equivalent approaches, particularly in systems with passivating behavior.

Methodologically, the results suggest using MEM and ST in combination with non-parametric detrending techniques, especially Wavelet or EMD, for analyzing EN signals affected by drift, transients, or non-stationary behavior. These combinations

offered the best balance between proximity to the reference value, statistical stability, and robustness to signal changes. Conversely, using signals without detrending or relying solely on SM can lead to biased estimates of V_c.

Overall, this study demonstrates that the accuracy of EN-based corrosion monitoring depends on the proper integration of preprocessing and spectral/time–frequency analysis. The developed factorial evaluation provides a methodological basis for selecting more reliable and reproducible combinations of analyses in metallic systems exposed to aggressive environments. Furthermore, the results contribute to the development of advanced non-invasive monitoring schemes, with potential applications in systems where the continuous acquisition of electrochemical signals can support decision-making for diagnosis, maintenance, and damage assessment.

As future work, it is recommended to extend this methodology to other passivable materials and corrosive media, as well as to incorporate cumulative thickness loss analysis for estimating remaining service life. It is also pertinent to evaluate automatic classification strategies based on machine learning or deep learning, using statistical, spectral, and time–frequency characteristics extracted from the EN signals as input. Finally, integrating these methods into embedded acquisition and processing systems would allow progress toward real-time monitoring platforms for corrosion diagnosis and prognosis.

These results provide a methodological basis for the design of more robust, traceable, and automatable electrochemical monitoring systems, especially in scenarios where signals exhibit drift, low signal–to–noise ratio, or transient behavior.

Acknowledgments

The authors acknowledge Tecnológico Nacional de México (TecNM) for the financial support provided through project No. 25687.26-PD, as well as Instituto Tecnológico Superior de Las Choapas (ITSCH), the home institution of **Oscar Jaime Ramos-Negrón**, **Jesús Francisco Solís-Alvarado**, **Limberg Morales-Clemente**, and **Cuauhtémoc Reyes-del-Valle**, for the institutional support provided during the development of this research. **Oscar Jaime Ramos-Negrón** and **Jorge Uruchurtu-Chavarin** acknowledges the Secretaría de Ciencia, Humanidades, Tecnología e Innovación (SECIHTI) for the support received. Likewise, **Oscar Jaime Ramos-Negrón** and **Jesús Francisco Solís-Alvarado** acknowledge the Programa para el Desarrollo Profesional Docente (PRODEP) for the support received in strengthening their academic and research activities. Finally, the authors acknowledge the Centro de Investigación en Ingeniería y Ciencias Aplicadas of the Universidad Autónoma del Estado de Morelos (CIICAp-UAEM) for the academic and scientific support provided.

References

Aballe, A., Bethencourt, M., Botana, F. J., & Marcos, M. (1999). Using wavelets transform in the analysis of electrochemical noise data. *Electrochimica Acta*, *44*(26), 4805–4816. https://doi.org/10.1016/S0013-4686(99)00222-4

Abdulmutaali, A., Aldrich, C., & Lepkova, K. (2025). Unsupervised process monitoring of corrosion based on electrochemical noise and multivariate image analysis. *npj Materials Degradation*, *9*, 43. https://doi.org/10.1038/s41529-025-00585-8

Arellano-Pérez, J., Escobar-Jiménez, R., Granados-Lieberman, D., Gómez-Aguilar, J., Uruchurtu-Chavarín, J., & Alvarado-Martínez, V. (2019). Electrochemical noise signals evaluation to classify the type of corrosion using synchrosqueezing transform. *Journal of Electroanalytical Chemistry*, *848*, 113249. https://doi.org/10.1016/j.jelechem.2019.113249

ASTM International. (2023). ASTM G102-23: Standard practice for calculation of corrosion rates and related information from electrochemical measurements. https://doi.org/10.1520/G0102-23

Avalle, Á., Bethencourt, M., Botana, F. J., & Marcos, M. (1999). Seguimiento de diferentes tipos de corrosión mediante la aplicación de la transformada de wavelets a registros de ruido en corriente. *Revista de Metalurgia*, *35*, 384–391. https://doi.org/10.3989/revmetalm.1999.v35.i6.647

Bertocci, U. [U.], Huet, F., Nogueira, R. P., & Rousseau, P. (2002). Drift removal procedures in the analysis of electrochemical noise. *Corrosion*, *58*(4), 337–347. https://doi.org/10.5006/1.3287684

Bertocci, U. [Ugo], Frydman, C., Gabrielli, C., Huet, F., & Keddam, M. (1998). Analysis of Electrochemical Noise by Power Spectral Density Applied to Corrosion Studies. *Journal of the Electrochemical Society*, *145*(8), 2780–2786. https://doi.org/10.1149/1.1838714

Botana-Pedemonte, F. J., Aballe-Villero, A., & Bárcena, M. M. (2002). *Ruido electroquímico: Métodos de análisis*. Septem Ediciones.

Box, G. E. P., Hunter, J. S., & Hunter, W. G. (2005). *Statistics for experimenters: Design, innovation, and discovery* (2nd ed.). John Wiley & Sons.

Cano, C., Romero, E., & Cubillos, G. I. (2023). Improvement of alkyd paints with NiO-ZrO_2Y coatings on hot-rolled steel. *Revista Mexicana de Ingeniería Química*, *22*(3). https://doi.org/10.24275/rmiq/Proc231

Cottis, R. (2001). Interpretation of electrochemical noise data. *Corrosion*, *57*(3), 265–285. https://doi.org/10.5006/1.3290350

Cottis, R., & Turgoose, S. (1995). Electrochemical noise measurements - a theoretical basis. *Electrochemical Methods in Corrosion Research V*, *192*, 663–672. https://doi.org/10.4028/www.scientific.net/MSF.192-194.663

Curso de corrosión básica. (2004). NACE International.

Escobar-Jiménez, R., Ramos-Negrón, O., Arellano-Pérez, J., & Campos, J. (2023). Short communication: Stockwell transform as an alternative method for the corrosion rate evaluation of 6061-t6 aluminum alloy. *Journal of Electroanalytical Chemistry*, *940*, 117493. https://doi.org/10.1016/j.jelechem.2023.117493

Esquivel-Rojas, A., Cuevas-Arteaga, C., & Valladares-Cisneros, M. G. (2020). Study of corrosion inhibition of copper in synthetic seawater by Equisetum arvense as green corrosion inhibitor. *Revista Mexicana de Ingeniería Química*, *19*(2), 603–616. https://doi.org/10.24275/rmiq/Mat629

Havashinejadian, E., Danaee, I., Eskandari, H., & Nikmanesh, S. (2017). Investigation on trend removal in time domain analysis of electrochemical noise data using polynomial fitting and moving average removal methods. *Journal of Electrochemical Science and Technology*, *8*(2), 115–123. https://doi.org/10.33961/JECST.2017.8.2.115

Homborg, A. M., Tinga, T., Westing, E. P. M., Zhang, Z., Ferrari, G. M., de Wit, J. H. W., & Mol, J. M. C. (2014). A critical appraisal of the interpretation of electrochemical noise for corrosion studies. *Corrosion*, *70*(10), 971–987. https://doi.org/10.5006/1277

Homborg, A. M., Tinga, T., Zhang, X., Van Westing, E. P. M., Oonincx, P. J., Ferrari, G. M., De Wit, J. H. W., & Mol, J. M. C. (2013). Transient analysis through Hilbert spectra of electrochemical noise signals for the identification of localized corrosion of stainless steel. *Electrochimica Acta*, *104*, 84–93. https://doi.org/10.1016/j.electacta.2013.04.085

Huang, J. Y., Qiu, Y. B., & Guo, X. P. (2010). Comparison of polynomial fitting and wavelet transform to remove drift in electrochemical noise analysis. *Corrosion Engineering, Science and Technology*, *45*(4), 294–298. https://doi.org/10.1179/147842208X338956

Huang, N. E., Shen, Z., Long, S. R., Wu, M. C., Shih, H. H., Zheng, Q., Yen, N.-C., Tung, C. C., & Liu, H. H. (1998). The empirical mode decomposition and the hilbert spectrum for nonlinear and non-stationary time series analysis. *Proceedings of the Royal Society of London A: mathematical, physical and engineering sciences*, *454*(1971), 903–995. https://doi.org/10.1098/rspa.1998.0193

Ikeuba, A. I., Njoku, C. N., Ekerenam, O. O., Njoku, D. I., Udoh, I. I., Daniel, E. F., Uzoma, P. C., Etim, I.-I. N., & Okonkwo, B. O. (2024). A review of the electrochemical and galvanic corrosion behavior of important intermetallic compounds in the context of aluminum alloys. *RSC Advances*, *14*(43), 31921–31953. https://doi.org/10.1039/d4ra06070a

Lavanya, M., Ghosal, J., & Rao, P. (2024). A comprehensive review of corrosion inhibition of aluminium alloys by green inhibitors. *Canadian Metallurgical Quarterly*, *63*(1), 119–129. https://doi.org/10.1080/00084433.2023.2190198

Lentka, Ł., & Smulko, J. (2019). Methods of trend removal in electrochemical noise data – overview. *Measurement*, *131*, 569–581. https://doi.org/10.1016/j.measurement.2018.08.023

Márquez-Herrera, A., Zapata-Torres, M., & Montesinos, S. (2026). Electrochemical engineering of passive films on AISI 304 stainless steel in H_2SO_4: The critical role of polarization slope in optimizing corrosion resistance. *Revista Mexicana de Ingeniería Química*, *25*(2). https://doi.org/10.24275/rmiq/Mat26765

Martínez-Ramos, C., Olguin-Coca, J., Lopez-Leon, L. D., Gaona-Tiburcio, C., Lara-Banda, M., Maldonado-Bandala, E., Castañeda-Robles, I., Jaquez-Muñoz, J. M., Cabral-Miramontes, J., Nieves-Mendoza, D., *et al.,* (2023). Electrochemical noise analysis using experimental chaos theory, power spectral density and hilbert–huang transform in anodized aluminum alloys in tartaric–phosphoric–sulfuric acid solutions. *Metals*, *13*(11), 1850. https://doi.org/10.3390/met13111850

Milošev, I. (2024). Corrosion inhibition of aluminium alloys by molybdate ions: A critical review of the chemistry, mechanisms and applications. *Corrosion Science*, *229*, 111854. https://doi.org/10.1016/j.corsci.2024.111854

Montgomery, D. C. (2012). *Design and analysis of experiments* (8th ed.). John Wiley & Sons.

Ramos-Negrón, O., Arellano-Pérez, J., Escobar-Jiménez, R., Gómez-Aguilar, J., & Granados-Liberman, D. (2019). Electrochemical noise analysis to identify the corrosion type using the stockwell transform and the shannon energy. *Journal of Electroanalytical Chemistry*, *836*, 50–61. https://doi.org/10.1016/j.jelechem.2019.01.020

Ramos-Negrón, O., Escobar-Jiménez, R., Arellano-Pérez, J., Uruchurtu-Chavarín, J., Gómez-Aguilar, J., & Lucio-García, M. (2019). Electrochemical noise analysis to identify the corrosion type using the stockwell transform and the shannon energy: Part ii. *Journal of Electroanalytical Chemistry*, 113597. https://doi.org/10.1016/j.jelechem.2019.113597

Roberge, P. R. [Pierre R.]. (2000). *Handbook of corrosion engineering* (2nd). McGraw-Hill.

Roberge, P. R. [Pierre R]. (2007). *Corrosion inspection and monitoring* (Vol. 2). John Wiley & Sons.

Roberge, P. R. [Pierre R.]. (2008). *Corrosion engineering principles and practice* (1st). McGraw-Hill.

Rodríguez-Yáñez, J., Uruchurtu-Chavarín, J., & Sanabria-Chinchilla, J. (2022). Tropical atmospheric corrosion of galvanized steel, in a light urban atmosphere in the San José valley of Costa Rica. *Revista Mexicana de Ingeniería Química*, *21*(2). https://doi.org/10.24275/rmiq/Mat2759

Schauer, T., Greisiger, H., & Dulog, L. (1998). Details on mem analysis of electrochemical noise data and correlation with impedance measurements for organic coatings on metals. *Electrochimica Acta*, *43*(16), 2423–2433. https://doi.org/10.1016/S0013-4686(97)10173-6

Stern, M., & Geary, A. L. (1957). Electrochemical polarization: I. a theoretical analysis of the shape of polarization curves. *Journal of The Electrochemical Society*, *104*(1), 56–63. https://doi.org/10.1149/1.2428496

Stockwell, R. G., Mansinha, L., & Lowe, R. P. (1996). Localization of the complex spectrum: The S transform. *IEEE Transactions on Signal Processing*, *44*(4), 998–1001. https://doi.org/10.1109/78.492555

Tukey, J. W. (1949). Comparing individual means in the analysis of variance. *Biometrics*, *5*(2), 99–114. https://doi.org/10.2307/3001913

Uruchurtu, J. C., & Dawson, J. L. (1987). Noise Analysis of Pure Aluminum Under Different Pitting Conditions. *Corrosion*, *43*(1), 19–26. https://doi.org/10.5006/1.3583104

Xia, D.-H., Deng, C.-M., Macdonald, D., Jamali, S., Mills, D., Luo, J.-L., Strebl, M. G., Amiri, M., Jin, W., Song, S., & Hu, W. (2022). Electrochemical measurements used for assessment of corrosion and protection of metallic materials in the field: A critical review. *Journal of Materials Science & Technology*, *112*, 151–183. https://doi.org/10.1016/j.jmst.2021.11.004